We are IntechOpen, the world's leading publisher of Open Access books Built by scientists, for scientists

6,900
Open access books available

186,000
International authors and editors

200M
Downloads

Our authors are among the

154
Countries delivered to

TOP 1%
most cited scientists

12.2%
Contributors from top 500 universities

WEB OF SCIENCE™

Selection of our books indexed in the Book Citation Index in Web of Science™ Core Collection (BKCI)

Interested in publishing with us?
Contact book.department@intechopen.com

Numbers displayed above are based on latest data collected.
For more information visit www.intechopen.com

15

The Use of Vibration Principles to Characterize the Mechanical Properties of Biomaterials

Osvaldo H. Campanella[1], Hartono Sumali[2], Behic Mert[3] and Bhavesh Patel[1]
[1]*Agricultural and Biological Engineering Department and Whistler Carbohydrate Research Center, Purdue University, West Lafayette, IN*
[2]*Sandia National Laboratories, Albuquerque, NM*
[3]*Department of Food Engineering, Middle East Technical University, Ankara*
[1,2]*USA*
[3]*Turkey*

1. Introduction

Mechanical properties are a primary quality factor in many materials ranging from liquids to solids including foods, cosmetics, certain pharmaceuticals, paints, inks, polymer solutions, to name a few. The mechanical properties of these products are important because they could be related to either a quality attribute or a functional requirement. Thus, there is always a need for the development of testing methods capable to meet various material characterization requirements from both the industry and basic research.

There is a wide range of mechanical tests in the market with a wide price range. However, there is an increasing interest in finding new methods for mechanical characterization of materials specifically capable to be adapted to in-line instruments. Acoustic/vibration methods have gained considerable attention and several instruments designed and built in government labs (e.g. Pacific Northwest National Laboratory and Argon National Laboratory) have been made commercially available.

To measure mechanical properties of material a number of conventional techniques are available, which in some cases may alter or change the sample during testing (destructive testing). In other tests the strains/deformations applied are so small that the test can be considered non-destructive. Both types of test are based on the application of a controlled strain and the measurement of the resulting stress, or viceversa. Different types of deformations, e.g. compression, shear, torsion are used to test these materials.

Depending on the type of material, different conventional techniques utilized to measure its mechanical properties can be grouped as viscosity measurement tests (liquid properties), viscoelasticity measurement tests (semiliquid/semisolid properties), and elastic measurement tests (solid properties).

Acoustics based techniques can be used for all types of material and the following sections discuss in detail how these techniques have been adapted and used to measure materials whose properties range from liquids to solids. Some of the applications discussed in this chapter are based on the basic impedance tube technique. Applications of this technique for

material characterization in air have been around for almost a century. The technique is described in basic acoustics text books such as Kinsler et al., (2000) and Temkin (1981). Impedance tube methods based on standing waves and the transfer function method have been accepted as standard methods by the American Society for Testing and Materials (ASTM 1990 and 1995), thus they will not be discussed in this chapter. Instead the chapter will focus on liquids, semiliquid and semisolid materials, many of them exhibiting viscoelastic properties, i.e. those properties that are more representative of biomaterials behavior.

2. Vibration fundamentals and analysis

The theoretical background that supports mechanical characterization of materials using vibration/acoustic based methods is mainly based on the characterization of acoustic waves propagating though the material. In that sense the analysis can be classified on the type of material being tested, i.e. liquid, viscoelastic semifluid, and viscoelastic semisolid.

2.1 Liquid materials

The analysis of liquid samples can be further classified based on the type of container used to confine the testing liquid. One of more important aspects to consider in this classification is the rigidity of the container walls. Two cases are considered: containers with rigid walls and containers with deformable/flexible walls.

2.1.1 Rigid wall containers

Since acoustic waves reveal useful information on the characteristic of the material through which they travel, measurement of acoustical properties such as velocity, attenuation, and phase changes resulting mainly from wave reflections in the transfer media are often used as a tool for mechanical characterization of materials. Specifically, ultrasound has found a wide range of applications in the measurement of the viscosity of liquids. Mason et al. (1949) first introduced an ultrasonic technique to measure the viscosity of liquids. They used the reflection of a shear wave in the interface between a quartz crystal and the sample liquid. Since then many other ultrasonics related techniques have been developed to measure viscosity of liquids [Roth and Rich (1953), Hertz et al. (1990), and Sheen et al., (1996)]. However, acoustical techniques that use sonic frequency have been rather limited. The main reason for this has been the lack of practical approaches that can employ frequencies in the sonic range to study the rheology of liquids. Tabakayashi and Raichel (1998) tried to use sonic frequency waves for rheological characterization of liquids. They affixed a hydrophone and a speaker to both ends of a cylindrical tube and analyzed the effect of the liquid non-Newtonian behavior on the propagation of the sound waves. The approach used by these authors is similar to the well known impedance tube method commonly applied to gases contained in cylindrical tubes, known as waveguides, but their analysis did not include the effect of the tube boundaries on sound propagation which can be of importance. In that sense, the application of the impedance tube techniques to test liquids has been limited because the loss of wall rigidity, i.e. the tube boundary, which normally it does not occur in tubes filled with air or air waveguides. Thus, when the tube is filled with a liquid, the tube may become an elastic waveguide and the rigid wall approximation loses its validity. The key assumption of having rigid walls is related to the shape of the acoustic

wave moving through the liquid. In order to have manageable equations to estimate the viscosity of the liquid from acoustic measurements using these systems it is important to generate planar standing waves from which acoustic parameters can be readily obtained. Mert et al. (2004) described a model and the experimental conditions under which the assumption of standing planar waves stands.

If a tube with rigid walls is considered the propagation of unidirectional plane sound waves though the liquid contained in the rigid tube can be described by the following equation (Kinsler et al., 2000):

$$\frac{\partial^2 p}{\partial t^2} - C_1^2 \frac{\partial^2 p}{\partial x^2} \tag{1}$$

where p is the acoustic pressure, t is time, x distance and C_1 the speed of the sound in the testing liquid. The solution of Equation (1) can be expressed in terms of two harmonic waves travelling in opposite directions and whose composition gives place to the formation of standing waves (Kinsler et al., 2000):

$$p(x,t) = p^{+} e^{\left[i\omega t + \hat{k}(L-x)\right]} + p^{-} e^{\left[i\omega t - \hat{k}(L-x)\right]} \tag{2}$$

p^+ is the amplitude of the wave traveling in the direction $+x$ whereas p^- is the amplitude of the wave traveling in the direction $-x$ and i is the imaginary number equal to $\sqrt{-1}$. The complex wave number $\hat{k} = \omega / C_1 - i\alpha$ includes the attenuation α due to the viscosity of the liquid, ω is the frequency of the wave. The corresponding wave velocity can be obtained from integration of the pressure derivative respect to the distance x, an equation that is known as the Euler equation (Temkin, 1981) and calculated as $v(x,t) = -\frac{1}{\rho_0}\int \frac{\partial p}{\partial x} dt$), which yields:

$$v(x,t) = P^{+} e^{\left[i\omega t + \hat{k}(L-x)\right]} - P^{-} e^{\left[i\omega t - \hat{k}(L-x)\right]} \tag{3}$$

By applying the boundary conditions such that at $x = 0$ the fluid velocity is equal to the velocity of the piston that creates the wave, which is $v(0,t) = v_0 e^{i\omega t}$. The other boundary condition is derived from the practical situation of using an air space on the other end of the tube, which mathematical provides a pressure release condition at $x = L$, written as $p(L, t) = 0$. With these boundary conditions the coefficients P^+ and P^- in Equation 3 can be calculated as:

$$P^{+} = \frac{\rho_0 C_1 v_0}{2\cos \hat{k} L} \quad \text{and} \quad P^{-} = -\frac{\rho_0 C_1 v_0}{2\cos \hat{k} L} \tag{4}$$

where ρ_0 is the density of the liquid, in repose, and v_0 the amplitude of the imposed wave.

An analysis made by Temkin (1981) showed that two absorption mechanisms produce the attenuation of the sound energy. One is due to the attenuation effects produced by the dilatational motion of the liquid during the acoustic wave passage. The other term arises from the grazing/friction motion of the liquid on the wall of the tube. It can be shown that the attenuation due to wall effects is significantly larger than the attenuation due to the

dilatational motion of the liquid (Herzfeld and Litovitz, 1959). Thus, a simplified form can be used to obtain the complex wave number ($\hat{k}$) and ultimately the attenuation (α) from which the fluid viscosity can be extracted. The complex wave number is given by the following equation:

$$\hat{k} = k_1 - i\alpha \tag{5}$$

where the real number k_1 is calculated as $k_1 = \frac{\omega}{C_1}$ and α is the attenuation of the wave due to the viscosity of the testing liquid.

For measurement purposes it is convenient to estimate the acoustic impedance as *p/v*, which from Equations (2) and (3) after application of the Fourier transform to the pressure and velocity variables yields:

$$Z_{a0} = \frac{\tilde{p}}{\tilde{v}} = \frac{i\rho_0\omega}{\hat{k}} \tan \hat{k}L = \frac{i\rho_0\omega}{\hat{k}} \frac{\sin \hat{k}L}{\cos \hat{k}L} \tag{6}$$

Where $\tilde{p}$ and $\tilde{v}$ are the Fourier transformed pressure and velocity respectively. The acoustic impedance is a complex number, as well as its inverse, which is known as mobility. Thus, the magnitude or absolute value of the mobility $Abs(1/Z_{a0})$ can be calculated. From values of the acoustic impedance or mobility the complex wave number $\hat{k}$ can be obtained as well as its real and imaginary components, from which the viscosity of the liquid and the intrinsic sound velocity in the liquid of interest can be estimated from the following equation (Temkin, 1981):

$$\hat{k} = k_1 - \frac{i}{RC_1}\left\{\left(\frac{\omega\mu}{2\rho}\right)^{0.5} + \left(\frac{\omega^2}{2C_1^2}\right)\left[\left(\frac{\mu}{\rho}\right)^{0.5} + \left(\frac{\mu}{3\rho}\right)^{0.5}\right] + \frac{\omega^2}{4C_1^2}\left(\frac{\mu}{\rho}\right)^{0.5}\right\} \tag{7}$$

Viscosities of the liquids can be also estimated from the Kirchhoff's equation, which has been derived for waveguides containing a gas and are given by the following equation (Kinsler et al., 2000):

$$\alpha = \frac{1}{RC_1}\sqrt{\frac{\mu\omega}{2\rho_0}} \tag{8}$$

The parameter *R* in Equations 7 and 8 is obtained from to the magnitude of the mechanical impedance at the resonance frequency (see Figure 2).

From Equation (6) can be observed that plots of the acoustic impedance becomes a maximum when $\cos(\hat{k}L)$ is a minimum, i.e. when the frequencies are given by the relationship $f = \frac{C_1}{2L}(n + \frac{1}{2})$, where n = 0,1,2,3,…., which is in terms of the length of liquid L and the velocity of sound in the liquid C_1, can provide a location of those maxima. Those theoretical observations were experimentally validated by Mert et al. (2004) using an experimental setup as that described in Figure 1.

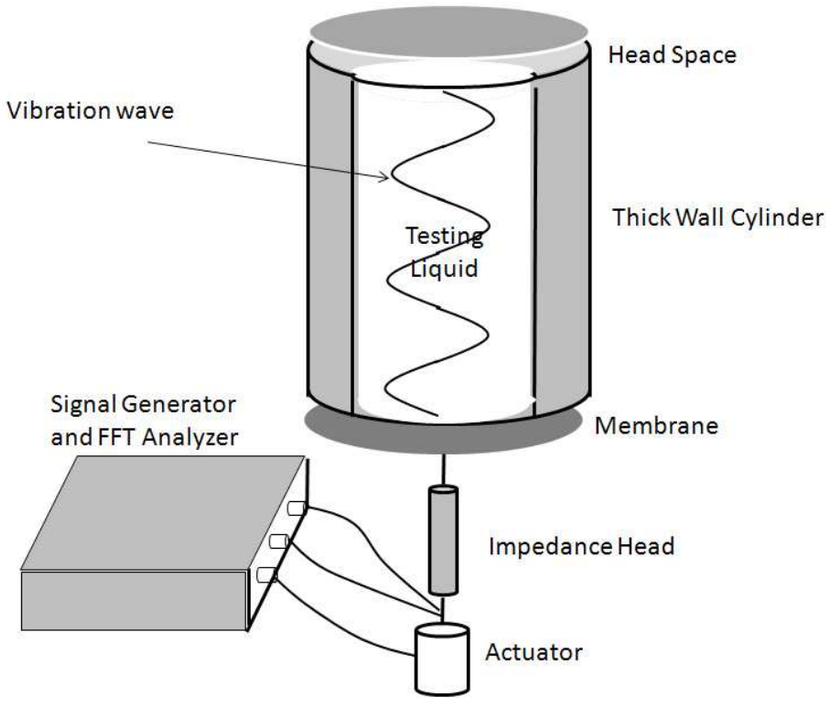

Fig. 1. Schematic of the apparatus to measure viscosity of liquids inside a thick wall rigid tube.

Further details of this experimental setting can be found elsewhere in Mert et al. (2004).
It has been hypothesized that plots of absolute mobility as a function of frequency should exhibit peaks and valleys corresponding to the resonance and anti-resonance frequencies of the standing waves from which the rheological properties of the liquid, notably its viscosity, can be obtained. To validate the theory described above, liquids with known physical properties including viscosity, density and sound velocity though them (the latter measured by a pulse-echo ultrasound method) were tested. Table 1 list viscosity of the liquids (liquids 1 to 4) used for this test along with their relevant physical properties.

Liquid	Viscosity *mPa . s*	Density kg/m^3	Intrinsic sound velocity *m/s*
1	17	800	1246
2	96	971	1010
3	990	969	967
4	4900	963	943
5	10,050	980	-

Table 1. Physical properties of the liquids used to validate theory; properties are at 25°C.

Figure 2 illustrates measured magnitude of the mechanical impedances Abs ($1/Z_{a0}$) liquids 2, 3, and 4 (see Table 1). It is clearly shown in the figure the effect of the liquid viscosity on the measured impedance, in general the higher is the viscosity of the liquid the lower is the value of the magnitude of the mechanical impedance at the peak/resonance frequency. The resonance frequency (frequency where peaks in impedance are obtained) is also affected by the viscosity of the liquid and tend to decrease when the viscosity of the liquid increases, which would be indicating a decrease in the sound velocity though the liquid. The latter in

fully agreement with the ultrasonic pulse-echo measurements used to estimate the sound velocities in the different liquids, which are reported in Table 1.

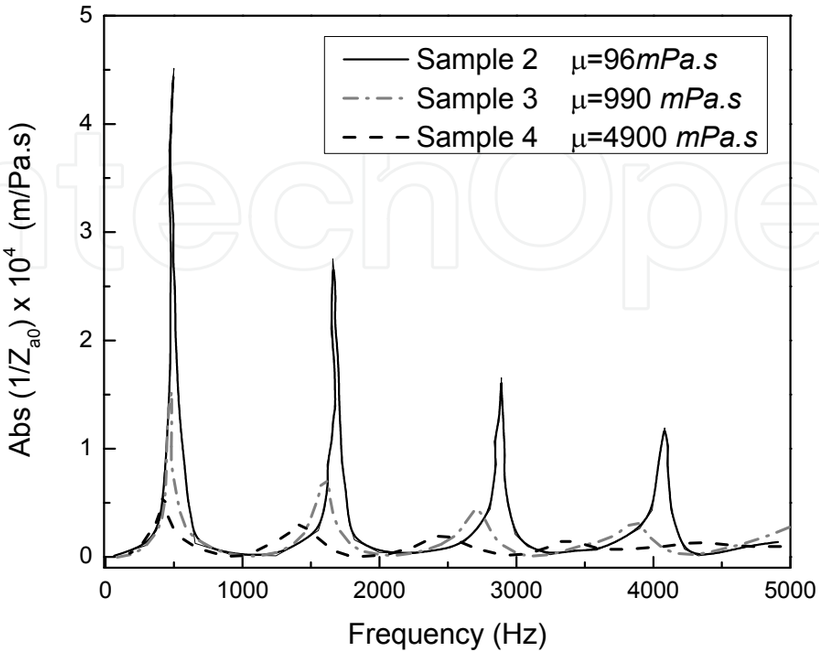

Fig. 2. Effect of viscosity on the magnitude of acoustical impedances measured in a setup as illustrated in Figure 1 at the driver position x = 0. Liquids 2, 3 and 4 were tested and properties and given in Table 1.

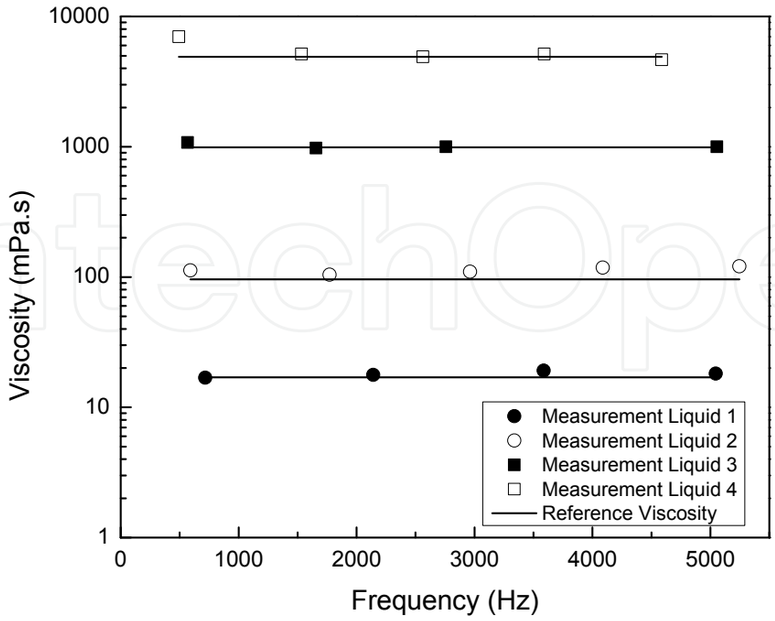

Fig. 3. Viscosities obtained from the different resonance frequencies for 4 different liquids obtained from the measured mechanical impedance and from Equation (7).

Extracted viscosities from impedance measurements along reported values of the liquid viscosities are illustrated in Figure 3.
Liquid viscosities were estimated from Equations 7 and 8 but better accuracy was obtained with Equation 7 that was derived for waveguides containing liquids (Mert et al., 2004). Results of the calculated viscosities are illustrated in Figure 3.

2.1.2 Flexible wall containers

When the walls of the waveguides are not rigid, during propagation of the waves the walls of the container expand and the overall liquid bulk modulus decreases leading to reduced sound velocity in the liquids. In addition, the fluid velocity cannot be assumed to be 0 at the can wall due to the expansion of the wall. These conditions make the governing equations used to estimate the wave attenuation and other relevant acoustic parameters very elusive, thus it is not possible estimate the liquid viscosity directly. One can overcome this problem by an empirical approach, which is by defining the quality factor *Q*, which is determined from the following equation:

$$Q = \frac{\omega_o}{\omega_2 - \omega_1} \tag{9}$$

ω_1 and ω_2 are the frequencies at which the amplitude of mechanical impedance response is equal to half the actual value at resonance and ω_0 is the resonance frequency (Kinsler et al., 2000). If the quality *Q* is known in a given container-liquid system it would be possible to have an estimation of the viscosity of the liquids contained in the container, which would serve for quality control purposes. To prove that concept Mert and Campanella (2007) performed a study where a shaker applied vibrations to a cylindrical can containing a liquid using a system, schematically shown in Figure 1. The vibration was able to move the can containing the liquid, and a wave was generated through the liquid, which reflected back in the interface between the liquid and the headspace to form standing waves resulting from composition of the forward and reflected wave. Properties of the standing waves were measured in the frequency domain, and in particular the resonance frequency and the amplitude of the wave at that resonant frequency were obtained and using a calibration curve approach related empirically to the rheological properties of the liquid. It is important to note that these measurements do not provide the true viscosity of the testing liquid because the walls of the can are not rigid and deform significantly due to the vibration. Despite of that the properties of the standing waves, measured by the quality *Q*, were highly correlated with the rheology of the liquid, which was tested offline in a rheometer (Mert and Campanella, 2007). Results shown in Figure 4 are a frequency spectra for the liquids reported in Table 1.
Quality factors *Q* for the testing liquids can be estimated from the two peaks observed in Figure 4 and potted as a function of the liquid viscosity as illustrated in Figure 5. However, as shown in Figure 4, the first resonances peaks do not seem to provide sufficient resolution and the second resonance peaks, at higher frequency, are used to find a relationship with the liquid viscosity.
Although interesting from an academic standpoint correlations like the one shown in the Figure 5 are not of practical applicability. However, if the can/cylinder contains a product

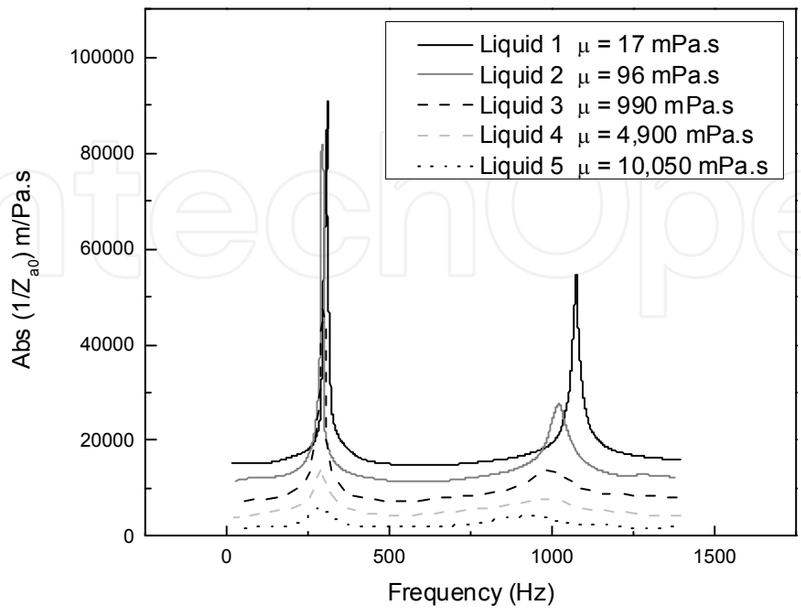

Fig. 4. Amplitudes at resonance frequencies for standard liquids given in Table 1. Curves were shifted up for clarity.

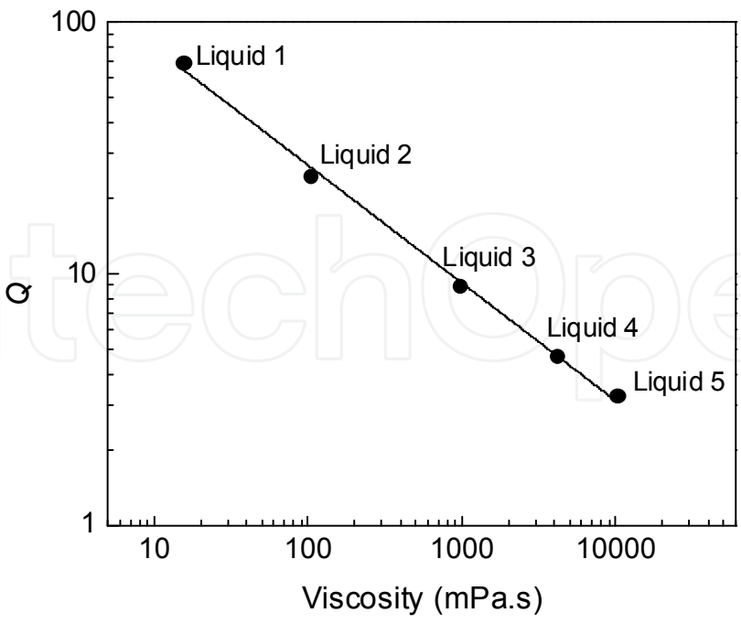

Fig. 5. Quality factor *Q* versus viscosity of liquid standards

whose viscosity is an important quality parameter, the present method would be of great applicability because the viscosity of the liquid could be assessed quickly without the necessity of opening the can (i.e. non-destructive method). One example of such application is testing cans of tomato products, which are widely produced and consumed in most part of the world and the viscosity of these products is a key parameter associated to their quality in terms of sensory evaluation and processing applications. Viscosity of tomato products is evaluated using a number of rheological techniques that range from empirical to more fundamental methods. One standard method is the use of the Brookfield^{TR} viscometer. This viscometer is based on the rotation of a particular element (spindle) inside a can containing the product. The viscosity of the product is obtained basically from the resistance offered by the product to the rotation of the spindle provided shear rates and shear stresses can be accurately calculated. Since the geometries of the spindles often are not regular it is difficult to estimate the rheological parameters, i.e. shear stress and shear rate, which enable the calculation of the liquid viscosity. Tomato paste is a very viscous product that exhibits an important structure that can be destroyed during testing. One approach to overcome this problem is the use of a helical-path spindle, which through a helical movement continuously is touching a fresh sample. Given the complicated rheology, results of this test are considered empirical. The other approach is to use technically advanced rheological equipment, which though the use of geometries such as parallel plates the sample can be minimally disturbed. For these cases the true viscosity of these tomato purees can be obtained. These materials are known as non-Newtonian to indicate that their viscosities are a function of the shear rate. Most of the non-Newtonian liquids can be described by a rheological model known as the power-law model which can be expressed by the following equation:

$$\eta = k\dot{\gamma}^{n-1} \tag{10}$$

where η is the apparent viscosity of the material, which is a function of the applied shear rate $\dot{\gamma}$ and k and n are rheological parameter known as the consistency index and the flow behavior , respectively. The value of k is an indication of the product viscosity whereas n gives a relation between the dependence of the viscosity with the applied shear rates. For tomato products n<1, and the smaller is the value of n the largest is the effect of the shear rate on the viscosity of the liquid. To test the feasibility of vibration methods, cans of tomato puree and dilutions ranging from 23% to 3.5% solids were tested in an apparatus similar to the one shown in Figure 1. Results of the tests can be observed in Figure 6, where frequency spectra resulting from some the tests are shown. Figure 7 shows possible correlations between the quality Q measured from the frequency spectra data and the parameter k determined using a standard rheological technique and a parallel plate geometry.

As indicated in Figure 6 the frequency spectra peaks shift to lower frequencies when the solid content of the concentrates increases. In the range of frequency tested the two peaks are visible for concentrates with low solid content whereas the second peak at higher frequencies disappears for concentrates with higher higher solid contents (23 Brix). The amplitude of the Absolute value of the mobility is considerably decreased when the solid content and the viscosity of the concentrate increase (Figure 6). Given the existence of two peaks quality values can be extracted from the two peaks and relate them with the measured rheological properties, in this case the value of the consistency index (Figure 7). It

can be seen in the figure that correlations of the liquid rheological properties with its acoustic properties measured by the quality factor Q are strong and that the quality evaluated at the first peak provides a better representation of the liquid viscosity. This is also enhanced due to the presence of two peaks for low and moderate solid contents (measured as Brix), which provides more experimental points to establish the correlation (see Figure 7 – and compare first peak and second peak data).

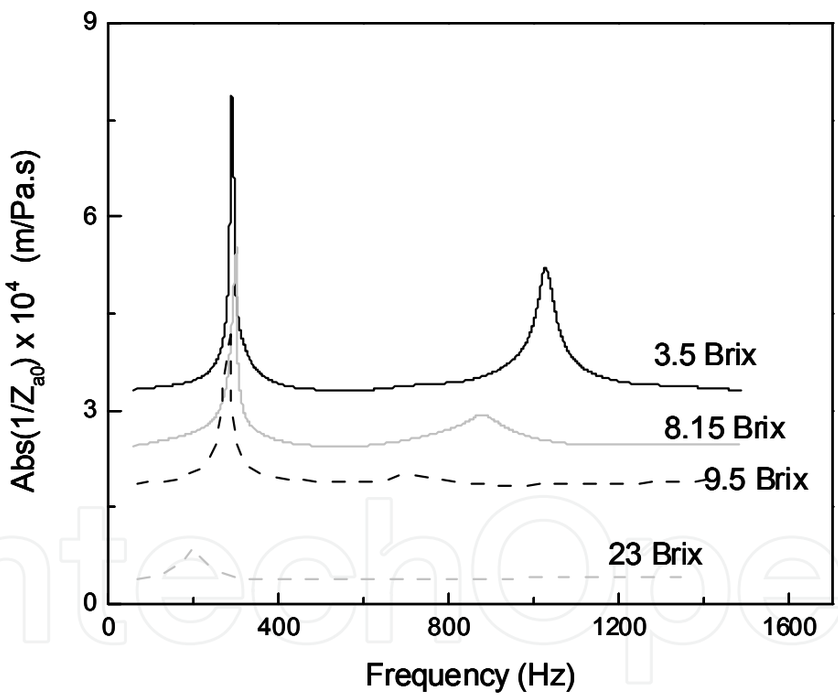

Fig. 6. Frequency response spectra of tomato concentrates at different soluble solids concentrations, measured as Brix. Curves were shifted up for clarity.

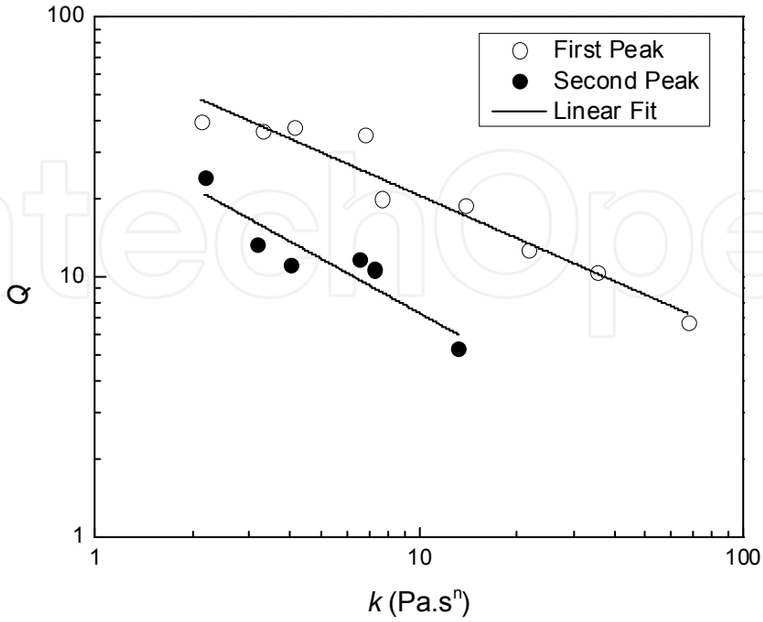

Fig. 7. Quality factor versus the consistency index *k* value for tomato puree and its dilutions

2.2 Viscoelastic materials

2.2.1 Semifluid materials

Squeezing flow is a well-known technique that has been applied to characterize the properties of various biomaterials ranging from liquids to semisolids. The traditional method involves measuring the force required to squeeze a sample between two cylindrical disks either at a constant velocity or by applying a constant force or stress (Campanella and Peleg 2002).

The oscillatory squeezing low method (OSF) uses the same geometry as the standard squeezing flow method but it involves the application of small amplitude oscillations at random frequencies up to 20 kHz (Mert and Campanella, 2008). The method allows one to calculate both the viscous and elastic components of the sample viscoelasticity by measuring the response of the material in terms of force and acceleration to those oscillations. Transformation of the measured force and acceleration to the frequency domain yields a frequency spectrum for the sample and, ultimately, its resonance frequency. From analysis of this frequency response, two important viscoelastic properties of the samples, the loss modulus G″ (viscous) and the storage modulus G′ (elastic), can be obtained.

The application of acoustic principles to the squeezing flow method is a novel technique, which convert the squeezing flow method into OSF methos can measure the rheological properties of materials that range from pure liquids to solids. Advantages of this method include it being non-invasive, little to no sample preparation, and its ability to monitor rapid changes during dynamic processes.

A schematic of the OSF testing apparatus is illustrated in Figure 8. The design uses a piezo-electric crystal stack attached to an impedance head. Upon the application of voltage, the upper plate oscillates, and the force and acceleration at the oscillating plate are measured

through the impedance head and transformed into the frequency domain using a Fast Fourier Transformation (FFT) routine. This transformation is very useful because from the inspection of the frequency response of the measurement it is possible to identify a characteristic resonance frequency for the sample.

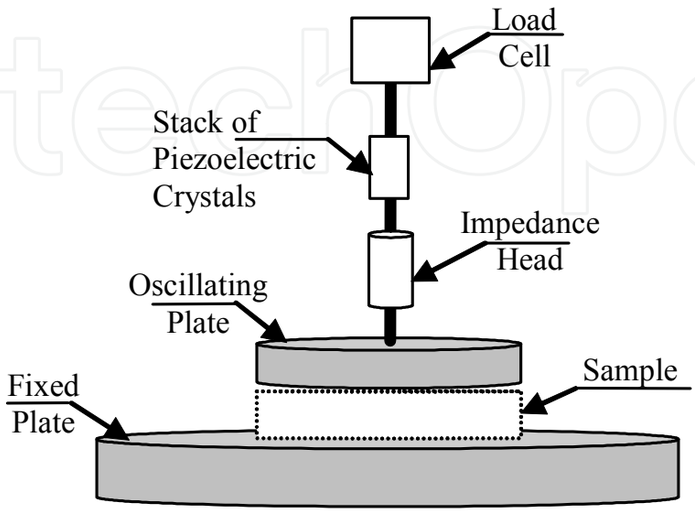

Fig. 8. Schematic of the OSF testing apparatus

Since the samples are considered viscoelastic they can be represented by a combination of elastic component, with a stiffness *S*, and viscous components with a damping *R*. A schematic of the elastic-viscous system used for analysis of the measurements is illustrated in Figure 9. For the testing, the sample is placed between the oscillating plate and a fixed plate. The oscillating plate is then brought down to touch the sample and the gap between

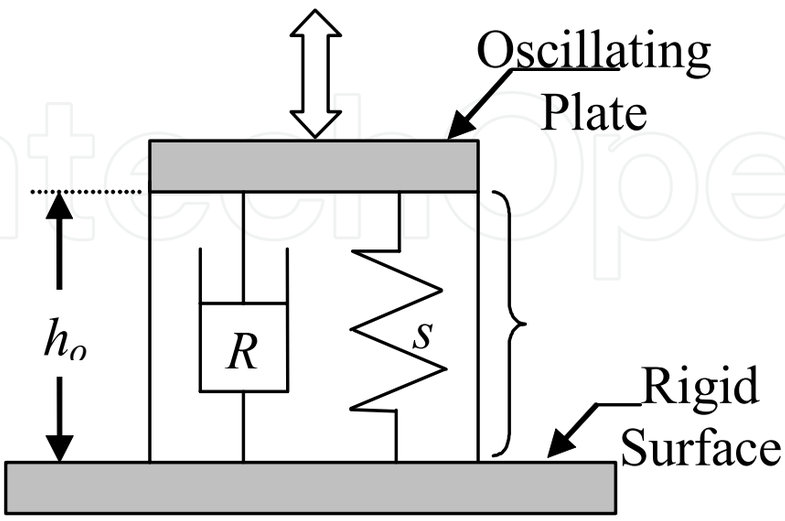

Fig. 9. Schematic of the spring-dashpot system, used for the analysis of the data. h_o, *R*, and *S* are the height, the viscous resistance (damping), and the stiffness of the sample respectively.

the plate (h_o) is noted. A load cell is attached above the oscillating plate to control the squeezing force applied to the sample prior the application of the oscillation. The squeezing force is simply applied to make sure that a good contact is established between the oscillating plate and the sample. It will be shown below, however, that the results are independent of that squeezing force.

The frequency response data is obtained using software that interfaces the results obtained with the signal generator device (see also details in Figure 1). The transformed mechanical impedance $\hat{Z} = \frac{\hat{F}}{\hat{u}}$ is then calculated from the force and velocity measured on the oscillating plate with the impedance head. $\hat{F}$ and $\hat{u}$ are the Fourier transformed variables and since they have been transformed into the frequency domain, they, as well as the mechanical impedance, are complex variables. The measured complex mechanical impedance at the driving point can be defined as:

$$\hat{Z}_{meas} = \hat{Z}_{instrument} + \hat{Z}_{sample} \tag{11}$$

where $\hat{Z}_{meas}$ is the measured impedance, $\hat{Z}_{instrument}$ is the instrument impedance that can be calculated simply as $\hat{Z}_{instrument} = im_{plate}\omega$ because the instrument does not have any spring mechanism or internal damping. From Equation (11) the sample impedance $\hat{Z}_{sample}$ can be obtained by subtracting the instrument impedance from the measured impedance.

The rheological behavior of the sample can be described in terms of the viscous component (R), which provides the damping of the oscillation and the elastic component (S), which provides the sample elasticity (Figure 9). The relationship between the mechanical impedance and the damping (viscous component) and stiffness (elastic component) of the sample can be described by Equation (12) below:

$$\hat{Z}_{sample} = R_{sample} + i \cdot (\omega \cdot m - \frac{S_{sample}}{\omega}) \tag{12}$$

where ω is the angular frequency of the oscillation, m is the mass of the system, and i is $\sqrt{-1}$.

The mobility of the sample, can be plotted as a function of frequency to provide the resonance spectrum of the sample. The resonance frequency, f_{res} of the sample, which is obtained as the frequency at which the mobility is a maximum is directly related to the stiffness and the mass of the system by Equation (13):

$$f_{res} = \sqrt{\frac{S_{sample}}{m}} \tag{13}$$

A typical plot of Mobility versus frequency for different concentrations of xanthan gum, a biopolymer that produces viscoelastic suspensions, is illustrated in Figure 10.

The higher is the concentration of xanthan gum the higher is its elasticity, which is clearly illustrated in the Figure 10 by a shifting to the right of the resonance frequency. That shifting of the frequency is a clear indication on increase in the stiffness of elasticity of the sample with concentration (see Equation 13).

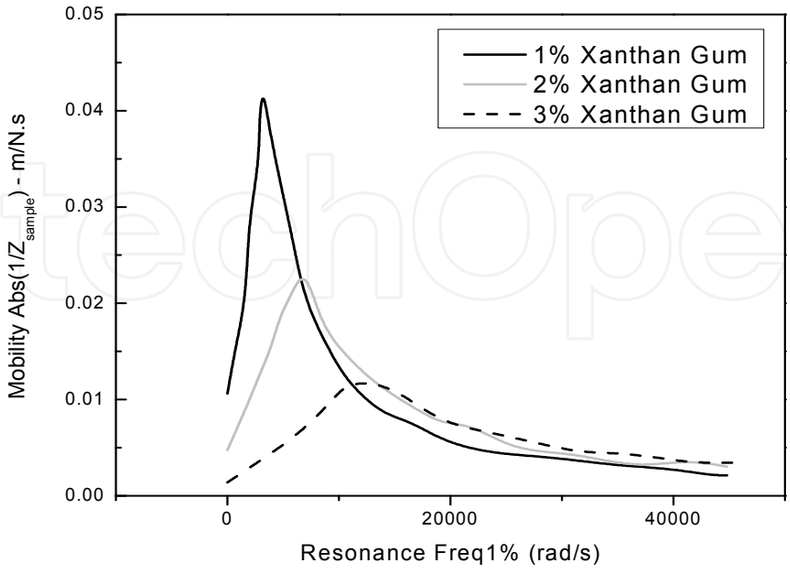

Fig. 10. Mobility plots obtained with the OSF method for xanthan gum dispersions of different concentrations

Although the mobility and the elastic and viscous components of a viscoelastic sample are often useful as quality and processing parameters (Gonzalez et al., 2010), for modeling purposes it is necessary to get quantitative and fundamental rheological information of a sample in terms of elastic and viscous modulus. Phan-Thien (1980) demonstrated that for viscoelastic materials subjected to squeezing flow under an oscillating plate, the squeezing flow force can be calculated as:

$$F_o \cos(\omega t) = \frac{3\pi a^4}{2h_o^3}\eta^* u_o \cos(\omega t) \tag{14}$$

where a is the radius of the top plate, h_o is the distance between plates and $\eta^* = \eta' - i\eta''$ is the complex dynamic viscosity of the sample. $\eta' = \frac{G''}{\omega}$ and $\eta'' = \frac{G'}{\omega}$ are the viscous and elastic components of the sample, respectively. Application of FFT to Equation (15) yields:

$$\hat{Z}_{sample} = \frac{3\pi a^4}{2h_o^3}\eta^* \tag{15}$$

Expressions can be rearranged and using the definition of the complex viscosity η^*, expressions for the viscoelastic moduli, i.e. the storage and loss modulus, G' and G'', can be obtained as:

$$G' = \left[Im\left(\hat{Z}_{sample}\right) + \frac{3m_{effective}\,\omega a^2}{20h_o^2} \right] \cdot \frac{2h_o^3\omega}{3\pi a^4} \tag{16}$$

$$G'' = Re\left(\hat{Z}_{sample}\right) \cdot \frac{2h_o^3 \omega}{3\pi a^4} \tag{17}$$

$Im\left(\hat{Z}_{sample}\right)$ and $\mathrm{Re}\left(\hat{Z}_{sample}\right)$ are the imaginary and real part, respectively, of the sample complex mechanical impedance $\hat{Z}_{sample}$. It is important to note that for the calculation of the storage modulus G' by Equation (16) is required to know the mass of the system, which consist of an effective mass that includes the mass of the sample and the squeezing force imposed to achieve good contact between the oscillating plate and the sample. If Equation (12) is rewritten in terms of those masses we can obtain an equation for the measured complex mechanical impedance:

$$\hat{Z}_{meas} = R_{sample} + i(\omega m_{plate} + \omega m_{effective} - S_{sample} / \omega) \tag{18}$$

The inertia produced by the plate instrument can be easily estimated as $\hat{Z}_{instrument} = i\omega m_{plate}$. However, to estimate the inertia produced by the effective mass $m_{effective}$ some additional calculations are required. If the imaginary part of the sample impedance is divided by the frequency, the following equation is obtained:

$$\frac{\mathrm{Im}(\hat{Z}_{sample})}{\omega} = (m_{effective} - S_{sample} / \omega^2) \tag{19}$$

The term S_{sample} / ω^2 in Equation (19) approaches to zero as the frequency is very high, which results in $\mathrm{Im}(\hat{Z}_{sample}) / \omega \approx m_{effective}$. Results of this calculation show that the parameter $\mathrm{Im}(\hat{Z}_{sample}) / \omega$ reaches an asymptotic value, which is independent of the squeezing force applied to the sample, S equals to $\mathrm{m_{effective}}$. That value can then be used to calculate the storage modulus by Equation (16). Results for a xanthan gum suspension of concentration 2%, and whose mobility versus frequency data is shown in Figure 10, are shown in Figure 11 in terms of the viscoelastic storage and loss moduli defined by Equations (16) and (17). As shown in the figure the data compares well with those obtained with a conventional rheometer at comparable frequencies. It must be also noted that the range of frequencies of the OSF method is significantly higher than those applied by conventional rheological methods where inertia may play an important role.

2.2.2 Semisolid materials

Physical properties of solid viscoelastic foods and other biological products are very important in food production, storage, handling, and processing. The importance of the knowledge of the physical properties of biomaterials is demonstrated in the case of fruits. One of the most important quality parameter of fruits is its texture. Texture is the first judgment a purchaser makes about the quality of a fruit, before sweetness, sourness, or flavor. Since fruit texture is such an important attribute, one would expect the changes in texture during maturation and cool-storage to be well understood, however this is not the case. One of the main limitations to the study of fruit texture is the accurate and precise measurement of texture as perceived by a consumer.

Traditionally, the texture of fruits is measured by a Magness Taylor pressure tester (Magness and Taylor, 1925). This simple device measures the force required to insert a metal

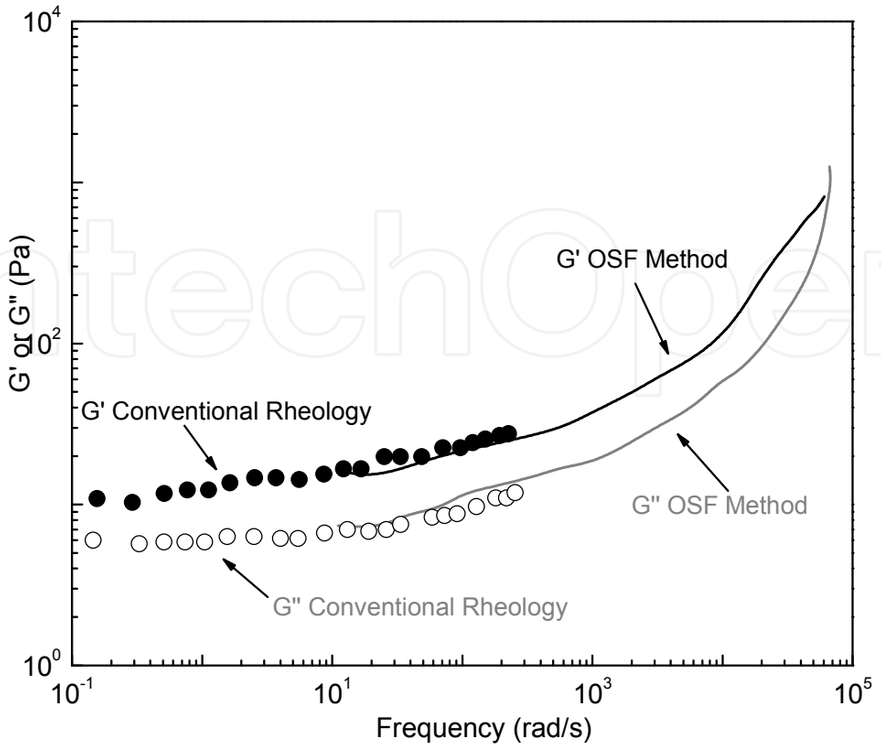

Fig. 11. Storage and loss modulus of a xanthan gum suspension of 2% concentration obtained with the OSF and conventional rheological methods

cylindrical plunger for a given distance into the fruit flesh. Although this device is cheap, quick, and easy to use, it has some disadvantages. Firstly, it is a destructive test, and it is not possible to have repeated measurements on a single fruit. Due to extremely high fruit-to-fruit variability, repeated measures on the same fruit would be highly desirable, especially from a research perspective. Secondly, there is high variability between operators, depending on the speed and force that the plunger is inserted into the fruit. However the greatest limitation of the Magness Taylor fruit pressure tester is that it measures the compression or crushing force that the cells of the fruit cortex are able to withstand. This force is very different from the force that is exerted on a fruit by the teeth of a consumer or the pressure that the consumer can exert with the fingers to assess the fruit texture. Biting an apple, for instance, involves cleaving cells apart, the exact opposite of the force measured by pressure testers. Universal Testing Machines (UTM), like for example the Instron™ instrument, are devices that can measure cleaving force, but they are slow, expensive, and again the method used with these machines is a destructive test.

Throughout the literature, there is abundant evidence that the ripeness or softness of intact fruits is related to their vibration properties. A device that uses vibrations to characterize intact fruits was patented in 1942 (Clark et al., 1942). Vibration properties of some fruits are correlated with firmness and ripeness. Finney (1970) explored methodologies for measuring and characterizing the vibration response of many fruits, and concluded that Young's modulus and shear modulus of apple flesh were correlated with the product between the resonance frequency squared and the mass of the whole fruit. It was also found that the

stiffness coefficient measured by vibration was closely associated with sensory panel subjective evaluations of Red Delicious apples (Finney, 1970, 1971). Garrett (1970) argued that the stiffness factor should be proportional to the frequency squared times mass to the two-thirds power. Cooke (1972) confirmed Garrett's theory using elastic theory relating the stiffness factor to the shear modulus of the fruit flesh. Both Finney's and Garrett's stiffness factors have been shown to correlate well with the fruit modulus (Clark and Shackelford, 1973; Yamamoto et al., 1980; and De Bardemaeker (1989); Abbott, 1994; Abbott and Liljedahl, 1994). Differences in shear moduli between green and ripe fruits can be detected non-destructively, and relatively easily, by vibration testing.

Through a few decades of development, a vibration-based characterization method called Experimental Modal Analysis (EMA) has advanced to become a very efficient tool for obtaining the dynamic properties such as natural frequency, damping and mode shapes in aerospace and mechanical engineering. For fruits, natural frequency is related to the shear modulus of the tissue (Cooke, 1972), which in turn determines the firmness of the fruit. For instance, in apples, high damping prevents them from giving a nice them from giving a nice crispy ringing sound when tapped (De Baerdemaeker and Wouters, 1987). Mode shapes are an important indicator of the whole fruit's conditions such as ripeness, bruises, or defects (Cherng, 2000). It is obvious that there is abundant information on the texture and quality of fruits that could be associated with their acoustic parameters. This section of the chapter is meant to give an idea of the direction that researchers have taken in the last decade or so. To give specific examples, a few details are given on the measurement of Young's modulus, finite element modeling, and experimental modal analysis.

2.2.2.1 Measuring modulus of elasticity

An instrument that measures force as a function of displacement, such as a UTM, can be used to obtain force-displacement curves of the samples. For a melon, the flesh and the rind should be tested differently. Melons have a rind that is significantly stiffer than the flesh. The cylindrical samples of the flesh can be tested with a compression test. The rind samples can be tested using a three point jig, and treated as a simply supported beam for analysis.

For modeling vibrations, where only small displacements are of interest, the tests should be limited to small displacements and changes in the cross-section and in the length can be ignored in the data processing. Also, the mechanical properties of biological materials in general are not constant. Because of the structures at the micro scale, the Young's modulus is a function of strain. The following method can be used to facilitate the computation of the Young's modulus at zero deformation. The stress-strain curve can be fit to a cubic function

$$\sigma = a_3\varepsilon^3 + a_2\varepsilon^2 + a_1\varepsilon + a_0 \tag{20}$$

The coefficients a_0 through a_3 can be obtained by cubic regression analysis. The Young's modulus is the derivative of the stress with respect to strain

$$E = \frac{d\sigma}{d\varepsilon} = 3a_3\varepsilon^2 + 2a_2\varepsilon + a_1 \tag{21}$$

For vibration analysis and modeling, the most important value of the Young's modulus is at zero strain, which is simply a_1. Therefore, the constitutive relation for vibration models is

$$\sigma = E\varepsilon \tag{22}$$

where $E = a_1$ from the test above.
In the bending test where the rind is treated as a simply supported beam, the equation for the young's modulus can be derived accordingly. If the force is applied in the middle of the span, then the deflection at that point is

$$x = \frac{FL^3}{48EI} \tag{23}$$

If the material is linear, the constant Young's modulus is

$$E = \frac{L^3}{48I}\frac{F}{x} \tag{24}$$

Where L is the span, and I is the moment of inertia of the rind sample, which is given by

$$I = \frac{base.height^3}{3} \tag{25}$$

For nonlinear materials, E can be obtained by taking the derivative of the force with respect to x. In particular, the Young's modulus at zero strain is

$$E(x) = \frac{L^3}{48I}\frac{dF}{dx}\bigg|_{x=0} \tag{26}$$

The modulus of elasticity of a melon was measured statically using an UTM machine, which can record the force as a function of deflection. For the flesh, cylindrical core samples were cut out of the melon; whereas for the rind, beam-like samples were cut out (Ehle, 2002). The force-displacement curve for the cylindrical core compression test was transformed into a stress-strain curve for small deflections by dividing the force by the cross-section area and dividing the deflection by the length. The small changes in cross-section area and the length were neglected because the displacement was small. Cubic regression of the stress-strain curve obtained the coefficients in Equation 20. Then Equation 21 was used to calculate the slope, which was the Young's modulus. The value at zero strain is the value used for modeling the vibration properties of the melon. Figure 12 shows that a cubic function fits the data very well, and that the slope at zero strain can be obtained accurately. In the above compression test of the flesh samples, the Young's modulus could also be obtained from the load-displacement curve without transforming into the stress-strain curve numerically. A little algebra gives:

$$E(x) = \frac{L}{A}\frac{df}{dx}\bigg|_{x=0} \tag{27}$$

For the bending test, the force-displacement data were processed according to Eq. 24 to obtain the Young's modulus of the rind. The result shows characteristics similar to those illustrated in Figure 12.

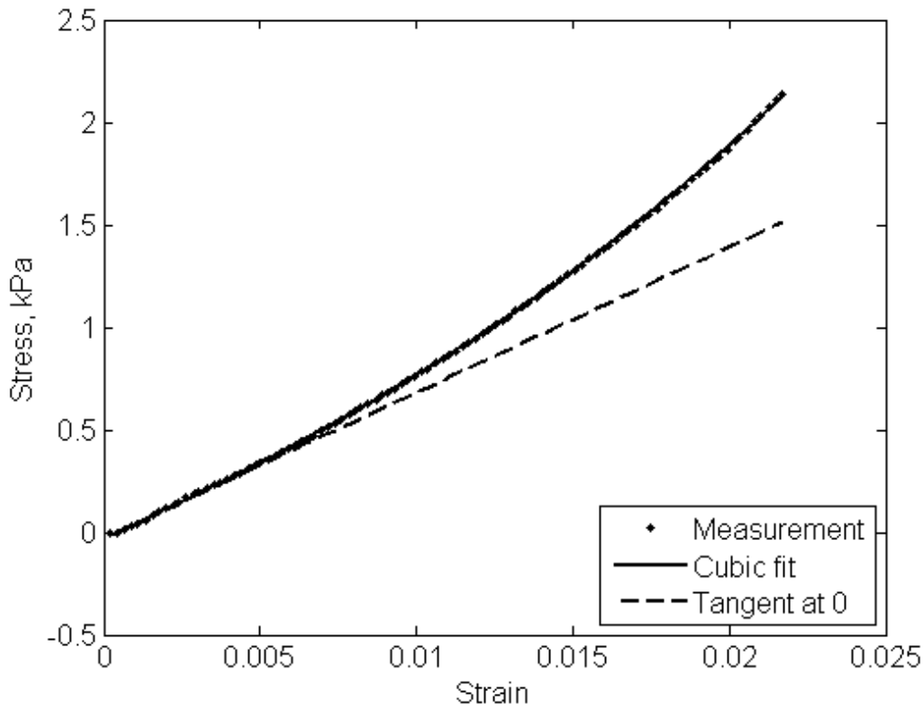

Fig. 12. Stress-strain curve of a core sample from compression test.

2.2.2.2 Numerical modal analysis with finite element modeling (FEM)

The application of stresses and strains in biological materials not only has a component associated to consumer evaluation but also it is related to quality control. Many of the stresses and strains are applied locally either during processing or consumption of the fruits. But they are distributed over the entire surface, thus it is necessary to use methods that can estimate the distribution of stresses over the product. Finite Element Modeling (FEM) is a well developed and proven mathematical and simulation tool to apply to the study of quality of fruits during consumption, storage and processing.

Cherng (2000) stated that the lowest natural frequency for hollow fruit like melons corresponded to the elongation along the major axis. Cooke (1972) concluded that the most important mode was the first twisting mode because it corresponds to the shear modulus of the flesh, which in turn corresponds to the fruit ripeness. Finite element models published in Cherng (2000) did not model the rind separately but assumed that the rind has the same properties as the flesh. Nourain et al (2004) compared a finite element model to experimental modal analysis results.

As an illustration, a finite element mesh used for a melon fruit is shown in Figure 13, with an octant removed to show the inside. The idealized melon-like geometry is a prolate ellipsoid with the major axis in the vertical direction. The major radius of the flesh is 77.5mm. The minor radius is 75mm. The hollow radii are 52.5mm (major) and 50mm (minor). The rind thickness is 2.5mm. For simulation purposes assumptions for the rind Young's modulus was 4.0 MPa whereas values used for the flesh Young's modulus were 1.0MPa, 1.5MPa, 2MPa, and 3MPa. The modal frequencies will be given in the order corresponding to those Young's moduli. The Young's moduli selected above are somewhat arbitrary and do not represent the values shown in Figure 12 from the test applied to a

melon. The purpose of this model is to give insight into how the vibration modes change with the stiffness of the flesh.

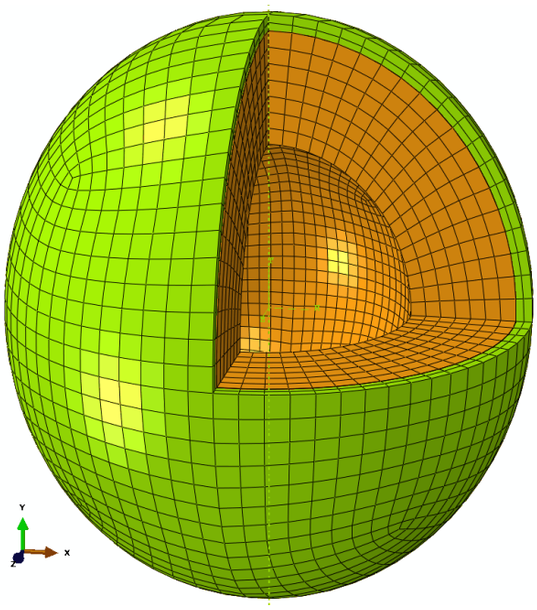

Fig. 13. A finite element mesh of a melon model

Figure 14 shows the elastic mode with the lowest natural frequency, which is elongation in the minor axis direction. Figure 15 shows the second mode, which is elongation in the major axis direction. Figure 16 shows the twisting mode. When the Young's modulus is 1.5MPa or lower, this mode changes shapes into the shape shown in Figure 17

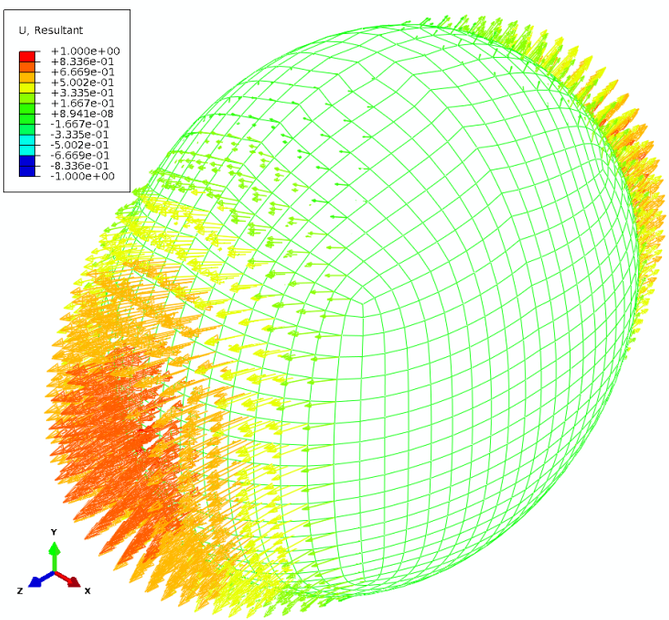

Fig. 14. Mode 1, "sideways elongation", 75.2Hz, 90.4Hz, 97.4Hz, 115.0Hz

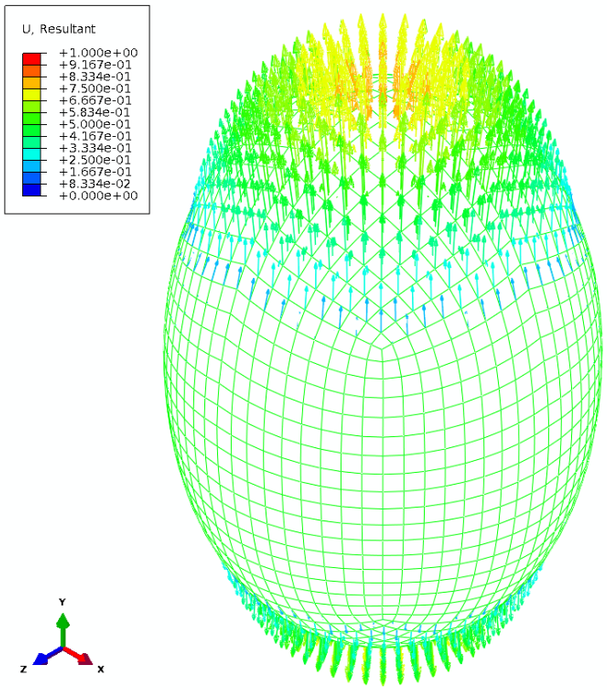

Fig. 15. Mode 2, elongation along the major axis, 79.4Hz, 91.5Hz, 102.0Hz, 120Hz

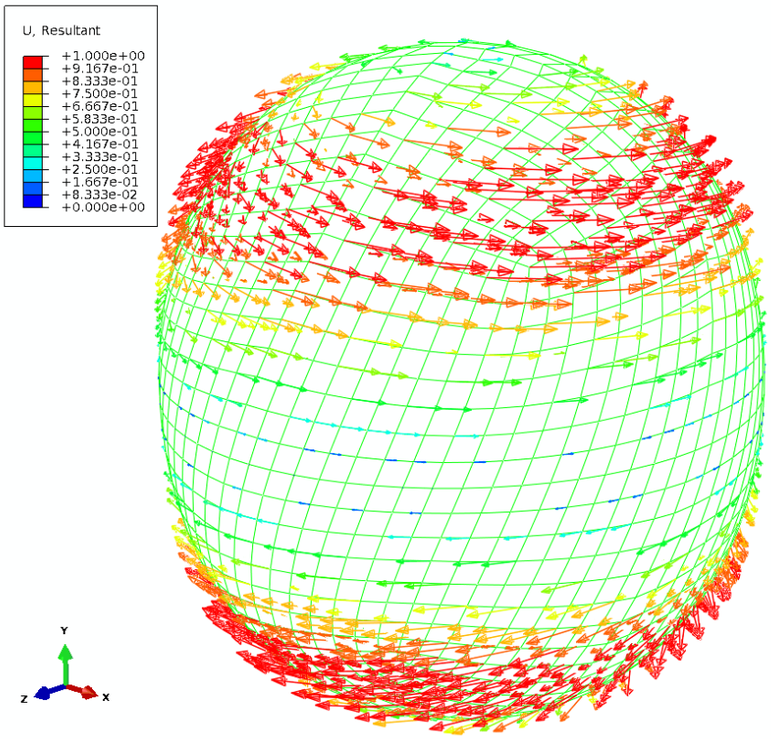

Fig. 16. Twisting about vertical axis, 101.4Hz, 125.1Hz, 135.0Hz, 152.3Hz

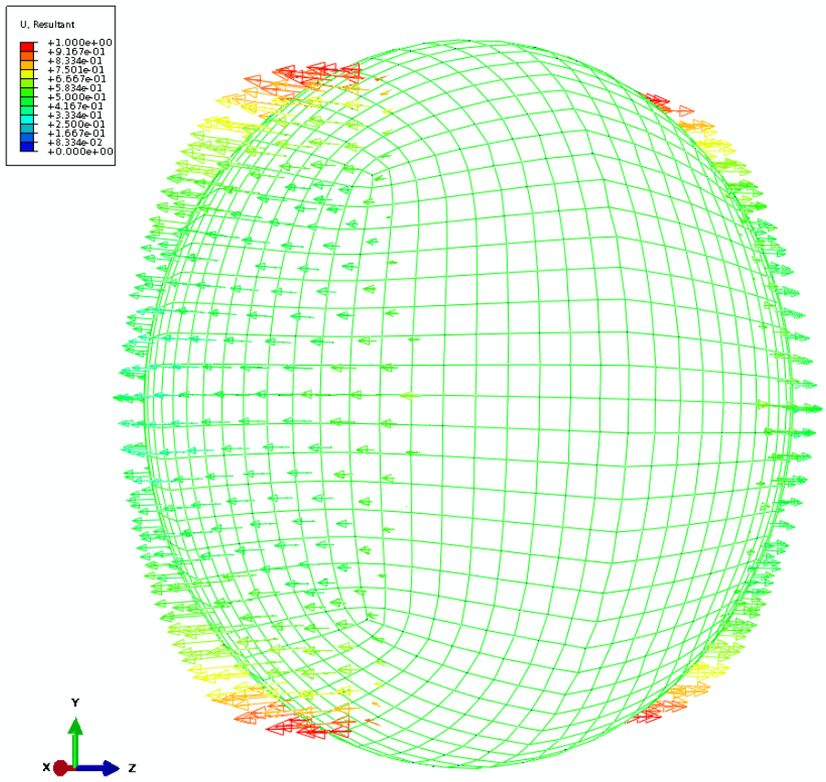

Fig. 17. Mode replacing the twisting mode when flesh Young's modulus is 1.5MPa

2.2.3 Experimental modal analysis of the fruit

Experimental modal analysis is a technique to obtain natural frequency, mode shapes and damping ratios of an elastic structure by application of a vibrational stimulus to the sample and sensing the resulting vibration at various locations on the sample surface. This section illustrates an experimental modal analysis on a melon fruit (Ehle, 2002). The excitation was a pulse force delivered by an impact hammer. A force transducer at the tip of the hammer measured the force. An accelerometer was used to measure the acceleration response at several points all over the surface of the melon. The measurement points were designed to follow a grid pattern where the distances between adjacent points were almost uniform throughout the surface of the fruit. The melon most closely resembled a sphere. Table 2 and Fig. 18 show the measurement points. A tri-axial accelerometer must be used to sense the important torsional mode (Fig. 8) as well as radial motions.

Layer	1	2	3	4	5	6	7	8	9
Points	1	2-7	8-19	20-37	38-55	56-73	74-85	86-91	92
Longitudinal Angle (deg)	90	67.5	45	22.5	0	-22.5	-45	-67.5	-90
Latitudinal Angle (deg)	N/A	60	30	15	15	15	30	60	N/A

Table 2. Locations of the points where acceleration was measured on the melon.

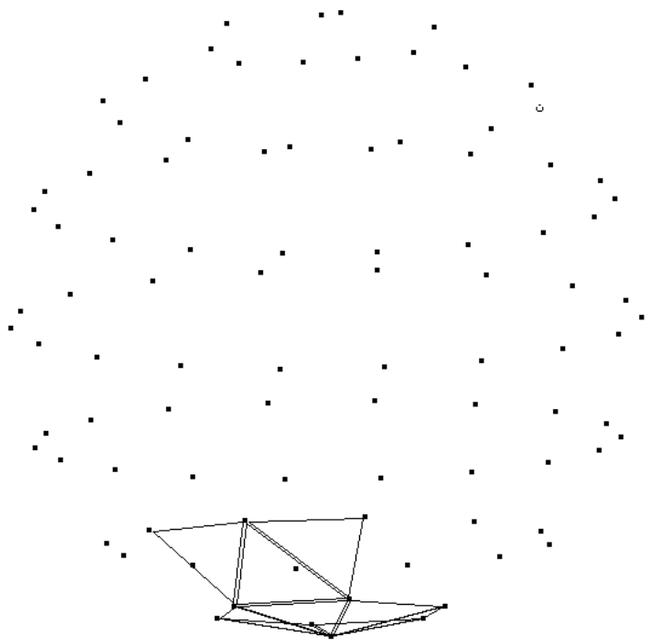

Fig. 18. Measurement points for the above described testing

Fig. 19. A long elastic cord and rubber bands supporting the melon.

Any method used to hold the melon is a boundary condition which will alter the vibration modes. However, the free-free boundary condition has been proven to not alter the vibration modes. This boundary condition can be approximated by suspending the melon from a rigid structure with elastic cords. Soft elastic cords are used in the suspension so that the rigid-body vibration of the melon and its suspension has very low natural frequency and does not alter the elastic modes. Figure 19 shows the suspension the setup used for the holding of the sample.

The porous surface of the melon made it difficult to affix the accelerometer to the surface of the melon using conventional methods. To make sure the accelerometer was affixed snugly to the surface of the melon, wax was applied to the bottom of the accelerometer. This allowed for the mating of the accelerometer to the surface of the melon, which would result in better vibration transmission. Also the accelerometer was held in place by a "cradle" made from rubber bands (Figure 20). The width of the rubber bands was approximately 6 mm, just wide enough to cover the top surface of the accelerometer. The rubber band was positioned in such a way as to apply sufficient pressure so that the surface of the accelerometer was always held normal to the surface of the melon. This configuration allowed for an effective and easy-to-move attachment method to install the accelerometer.

Fig. 20. Accelerometer attachment

To excite the fruit a modal hammer with a force transducer was used. A plastic tip was used as opposed to the metal tip. The plastic tip allowed for the force from the hammer to stay within the crucial 20dB range past the cut off frequency of 500 Hz. The accelerometer then measured the resulting accelerations of the surface of the melon. An FFT analyzer transformed the acceleration and force into the frequency domain, and obtained the ratio of acceleration to force, which was the Frequency Response Function (FRF) at each sense point.

To reduce random noise, the average of data from ten impacts was used to compute each FRF. The *coherence* is a function in the frequency domain that indicates the quality of the FRF. A perfect coherence is 1.0. A coherence less than that at a given frequency means that the vibration sensed by the accelerometer at that particular frequency is not a linear response to the excitation from the impact hammer. A low coherence in general indicates excessive noise, nonlinearity, or other causes of bad measurement.

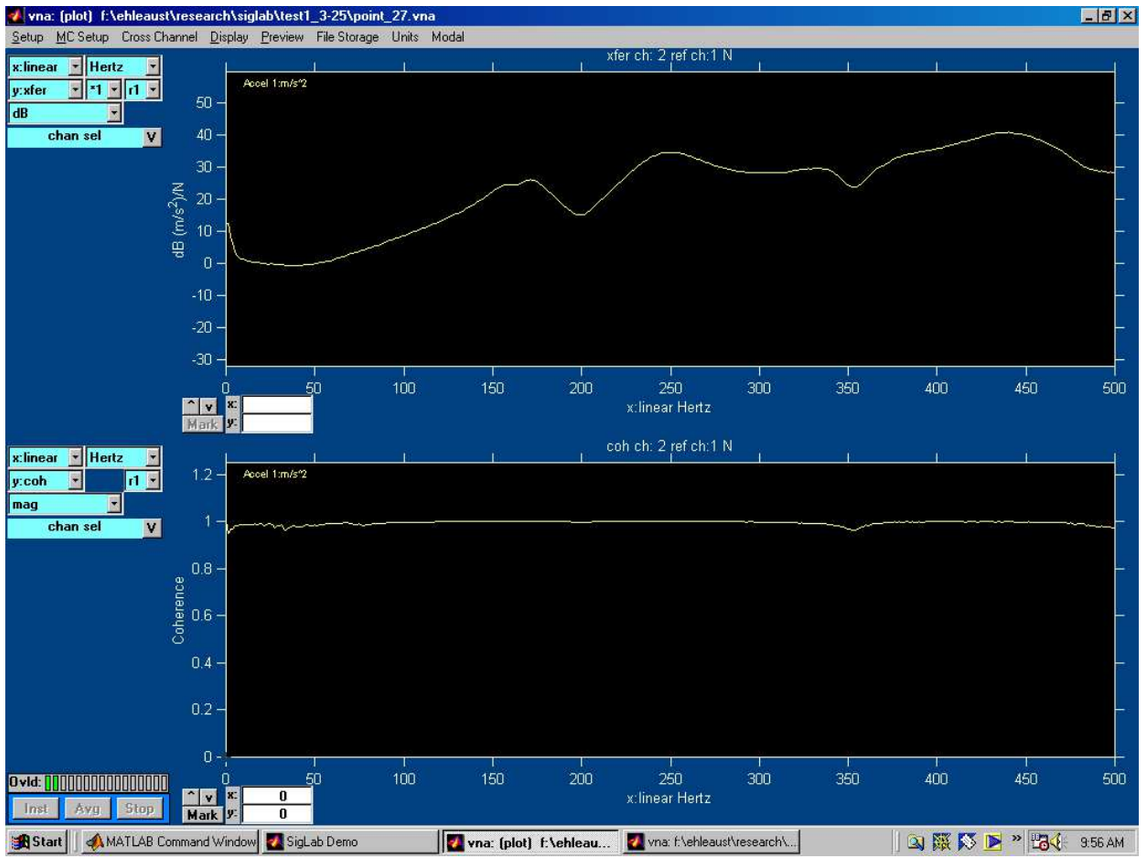

Fig. 21. Frequency response function obtained by hitting the melon rind directly

Figure 11 shows a typical FRF (top curve) and coherence (bottom curve) from the measurement. Each measurement point in Table 1 resulted in one FRF. A peak at a certain frequency means large vibration at that frequency, which indicates a mode at that frequency. If the FRF at a particular point shows a valley or low response at a modal frequency, it is indicating that the point is a node (point of no motion) of the corresponding mode shape. Using those rules, the mode shapes at any resonant frequency could be visually determined. A modal analysis program uses mathematical algorithms to compute the natural frequency, damping and mode shapes from the FRFs. It was used to analyze data from this test, but may not be necessary if the tester can figure out the modes by careful visual examination of the FRFs.

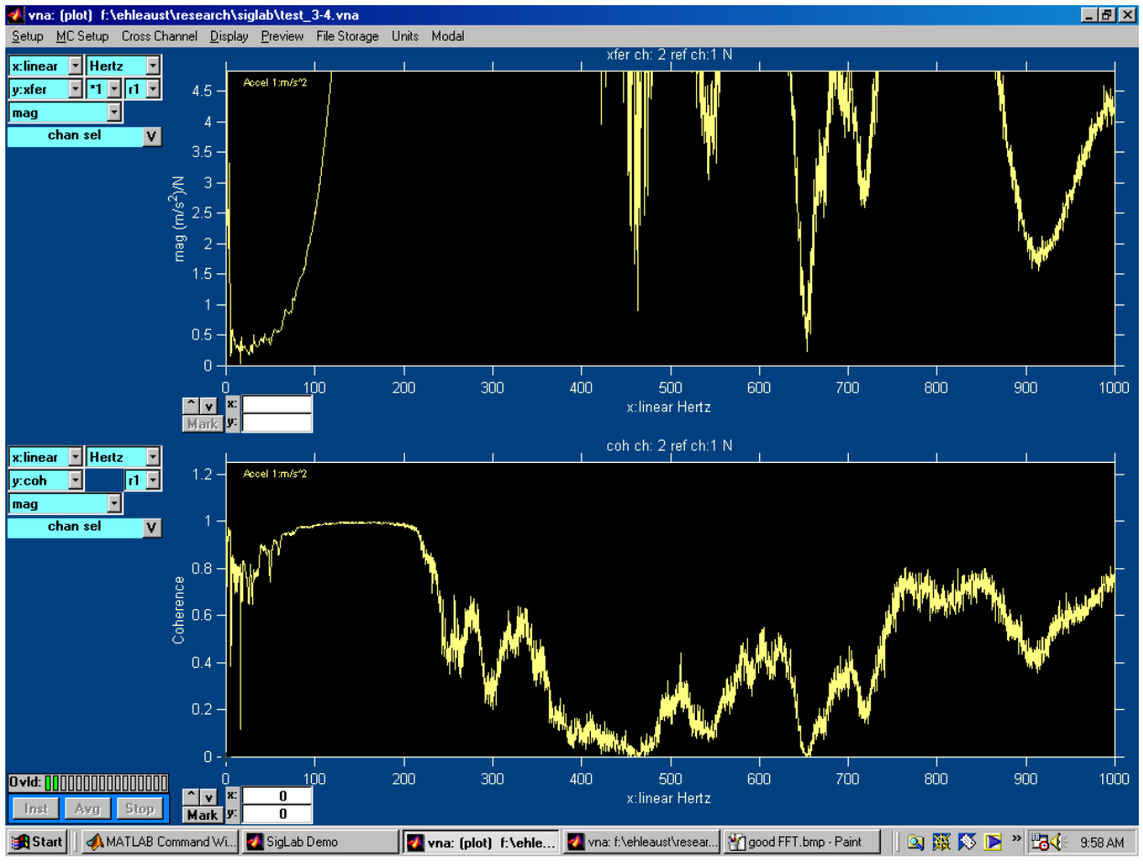

Fig. 22. An FRF (top) and coherence (bottom) obtained without a local stiffener on the surface of the melon.

Fig. 23. A stiffening metal disk on the melon rind.

It is important that the excitation force contain energy at all the frequencies of interest. That means that the force imparted by the hammer on the fruit must be a sharp enough pulse in the time domain. Experimental modal analysis is most commonly done on hard structures such as vehicles, buildings or metal structures. The surface of the fruit is much softer than most other structures for which the hammer tip was designed. Hitting the fruit with a hammer would result in a broad pulse in time domain, which translates into a narrow-band excitation in the frequency domain. As a result, the impulse spectrum of the excitation force would not have enough energy to excite vibration modes higher than 200 Hz without its intensity dropping more than 20 dB from its DC magnitude. When that condition is violated, the coherence of the data is very poor as seen in figure 22. To overcome this narrow-band excitation problem, a small metal disk (Figure 23) was attached to the fruit at the point of impact. This resulted in a significantly broader-band force excitation.

3. Concluding remarks

This chapter has presented a few examples of research that has been done to take advantage of the advancement in vibration analysis along with applications to characterize the rheological properties of biomaterials. The literature shows that the rheological properties of biomaterials are associated to quality indicators, specifically for foods to their texture and their sensory evaluation, thus many of the applications described in this chapter deal with food materials. In particular, this chapter has shown examples of application of basic vibration theories to measure the rheology of liquids as well as viscoelastic semi fluids and semi solid materials. The static measurement of modulus, finite element computation of the vibration natural frequencies and mode shapes, and an experimental modal analysis of a melon fruit are also described.

The authors believe that research on testing of biomaterials using vibration methods may help achieve:

- Higher quality foods due to better selection, testing, handling, grading and processing
- Lower prices due to quick nondestructive tests in harvesting, selection and grading of raw materials as well as testing finished products like for example during canning operations
- Increase in food safety due to, for example, the ability to detect dangerous salmonella in eggs from the change in physical properties detected by quick and accurate vibration based methods (Sinha et al., 1992) or infestation in fruits.
- Better design of food packaging, handling and transportation.
- Better tools to monitor the rheological properties of raw materials, e.g. during cooking and drying of cereal (Gonzalez et al., 2010)
- More interdisciplinary research combining engineering and food and biological sciences.

4. References

Abbott, J.A., (1994). Firmness measurement of freshly harvested delicious apples by sensory methods, sonic transmission, magness-taylor, and compression. Journal of American Society of Horticultural Science, 119(3), 510-515.

Abbott, J.A., Liljedahl, L.A., (1994). Relationship of sonic resonant frequency to compression test and magness-taylor firmness of apples during refrigerated storage. Transactions of the ASAE, 37(4), 1211-1215.

American Society for Testing and Materials, (1995). Standard test method for impedance and absorption of acoustical materials by the impedance tube method. ASTM Designation: C, 384-95.

American Society for Testing and Materials, (1990). Standard test method for impedance and absorption of acoustical materials using a tube, two microphones, and a digital frequency analysis system, ASTM Designation: E, 1050-90.

Campanella, O.H., Peleg, M., (2002). Squeezing flow viscometry for nonelastic semiliquid-foods theory and applications. Critical Reviews in Food Science and Nutrition, 42(3), 241–264.

Chen, H., De Baerdemaeker, J., (1993). Modal analysis of the dynamic behavior of pineapples and its relation to fruit firmness. Transactions of the ASAE, 36(5), 1439-1444.

Cherng, P.A., (2000). Vibration modes of ellipsoidal shape melons. Transactions of the ASAE, 43(5), 1185–1193.

Clark, H.L., Lake, B., Mikelson, W., (1942). Fruit ripeness tester, U.S. Patent 2277037.

Clark, R.L., Shackelford, P.S., (1973). Resonant and Optical Properties of Peaches as Related to Flesh Firmness. Transactions of the ASAE, 16(6), 1140-1142.

Cooke, J.R., (1972). An interpretation of the resonant behavior of intact fruits and vegetables. Transactions of the ASAE, 15(4), 1075-1080.

De Baerdemaeker, J., Wouters, A., (1987). Mechanical properties of apples: II. Dynamic measurement methods and their use in fruit quality evaluation, In: Jowitt R.

(Eds). Physical properties of foods 2, Elsevier Applied Science, Pp.417-428, London , U.K.,

Ehle, A., (2002). Measuring modulus of elasticity and vibration modes of a melon. Undergraduate Research Report, (unpublished), Purdue Univerisity, West Lafayette, IN, USA.

Finney, E., (1970). Mechanical resonance within red delicious apples and its relation to fruit texture. Transactions of the ASAE, 13(2), 177-180.

Finney, E., (1971). Dynamic elastic properties and sensory quality of apple fruit. Journal of Texture Studies, 2, 62-74.

Garrett, R.E., (1970). Velocity of Propagation of Mechanical Disturbance in Apples, PhD Thesis, Cornell University, Ithaca, New York.

D.C. Gonzalez, D.C, Khalef, N., Wright, K, Okos,M.R., Hamaker, B.R and Campanella, O.H. (2010). Physical aging of processed fragmented biopolymers. Journal of Food Engineering, 100(2), 187-193.

Hertz, T.G., Dymling, S.O., Lindstrom, K.,. Persson, H.W., (1990). Review of Scientific Instruments, 62, 457.

Herzfeld, F.K., Litovitz, T.A, (1959). Absorption and Dispersion of Ultrasonic Waves. Academic Press, New York.

Kinsler, L.E., Frey, A.R., Coppens, A.B. and Sanders, J.V., (2000). Fundamentals of Acoustics (4th edn). John Wiley and Sons, Inc, New York.

Magness, J.R., Taylor, G.F., (1925). An improved type of pressure tester for the determination of fruit maturity. USDA Agri. Circular , 350, Pp.8. Washington, D.C., USDA.

Mason, W.P., Baker, W.O., McSkimin, H.J., Heiss, J.H., (1949). Measurement of shear elasticity and viscosity of liquids at ultrasonic frequencies. Phys. Rev. 75, 936.

Mert, B., Campanella, O.H., (2007). Monitoring the rheological properties and solid content of selected food materials contained in cylindrical cans using audio frequency sound waves. Journal of Food Engineering, 79 (2), 546-552.

Mert, B., Campanella, O.H., (2008). The study of the mechanical impedance of foods and biomaterials to characterize their linear viscoelastic behavior at high frequencies. Rheologica Acta, 47, 727-737.

Mert, B., Sumali, H., Campanella, O.H., (2004). A new method to measure viscosity and intrinsic sound velocity of liquids using impedance tube principles at sonic frequencies. Review of Scientific Instruments, 75(8), 2613–2619.

Nourain, J., Ying, Y.B., Wang, J., Rao, X., (2004). Determination of acoustic vibration in watermelon by finite element modelling. Proceding of SPIE, 5587, 213, doi:10.1117/12.576953

Phan-Thien, N.,(1980). Small strain oscillatory squeeze film flow of simple fluids. Journal of the Australian Mathematical Society (Ser. B), 32, 22–27.

Roth,W., Rich, S.R., (1953). A new method for continuous viscosity measurement. General theory of the ultra-viscoson. Journal of Applied Physics, 24, 940-950

Sheen, S.H., Chein, H.T., Rapis, A.C., (1996). Measurement of shear impedances of viscoelastic fluids, IEEE Ultrasonic Symposium Proceedings, IEEE, New York.1, pp. 453.

Sinha, D.N. Johnston, R.G. Grace, W.K., Lemanski, C.L., (1992). Acoustic resonances in chicken eggs. Biotechnology Progress, 8, 240-243.

Takabayashi, K., Raichel, D.R., (1998). Discernment of non-Newtonian behavior in liquids by acoustic means, Rheol. Acta, 37, 593–600.

Temkin, S., (1981). Elements of Acoustics. John Wiley and Sons, New York.

Yamamoto, H.M., Iwamoto, M., Haginuma, H., (1980). Acoustic Impulse Response Method for Measuring Natural Frequency of Intact Fruits and Preliminary Applications to Internal Evaluation of Apples And Watermelons. Journal of Texture Studies, 11, 117-136.

IntechOpen

IntechOpen

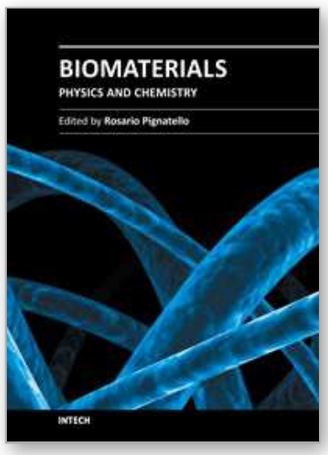

Biomaterials - Physics and Chemistry
Edited by Prof. Rosario Pignatello

ISBN 978-953-307-418-4
Hard cover, 490 pages
Publisher InTech
Published online 14, November, 2011
Published in print edition November, 2011

These contribution books collect reviews and original articles from eminent experts working in the interdisciplinary arena of biomaterial development and use. From their direct and recent experience, the readers can achieve a wide vision on the new and ongoing potentialities of different synthetic and engineered biomaterials. Contributions were selected not based on a direct market or clinical interest, but based on results coming from very fundamental studies. This too will allow to gain a more general view of what and how the various biomaterials can do and work for, along with the methodologies necessary to design, develop and characterize them, without the restrictions necessarily imposed by industrial or profit concerns. The chapters have been arranged to give readers an organized view of this research area. In particular, this book contains 25 chapters related to recent researches on new and known materials, with a particular attention to their physical, mechanical and chemical characterization, along with biocompatibility and hystopathological studies. Readers will be guided inside the range of disciplines and design methodologies used to develope biomaterials possessing the physical and biological properties needed for specific medical and clinical applications.

How to reference
In order to correctly reference this scholarly work, feel free to copy and paste the following:

Osvaldo H. Campanella, Hartono Sumali, Behic Mert and Bhavesh Patel (2011). The Use of Vibration Principles to Characterize the Mechanical Properties of Biomaterials, Biomaterials - Physics and Chemistry, Prof. Rosario Pignatello (Ed.), ISBN: 978-953-307-418-4, InTech, Available from: http://www.intechopen.com/books/biomaterials-physics-and-chemistry/the-use-of-vibration-principles-to-characterize-the-mechanical-properties-of-biomaterials

INTECH
open science | open minds

InTech Europe
University Campus STeP Ri
Slavka Krautzeka 83/A
51000 Rijeka, Croatia
Phone: +385 (51) 770 447
Fax: +385 (51) 686 166
www.intechopen.com

InTech China
Unit 405, Office Block, Hotel Equatorial Shanghai
No.65, Yan An Road (West), Shanghai, 200040, China
中国上海市延安西路65号上海国际贵都大饭店办公楼405单元
Phone: +86-21-62489820
Fax: +86-21-62489821

© 2011 The Author(s). Licensee IntechOpen. This is an open access article distributed under the terms of the Creative Commons Attribution 3.0 License, which permits unrestricted use, distribution, and reproduction in any medium, provided the original work is properly cited.

IntechOpen

IntechOpen